AGU PUBLICATIONS

Geophysical Research Letters

RESEARCH LETTER
10.1002/2016GL068904

Key Points:
- Dendritic network models substantially improve isoscapes of strontium isotopes in rivers
- Models can quantify influence of landscape versus in-stream driven processes on isotopes in rivers
- Landscape and in-stream processes shape strontium isotopes in rivers at multiple spatial scales

Supporting Information:
- Supporting Information S1
- Table S1
- Table S2
- Table S3
- Table S4
- Table S5
- Table S6
- Table S7

Correspondence to:
S. R. Brennan,
srbrenn@uw.edu

Citation:
Brennan, S. R., C. E. Torgersen, J. P. Hollenbeck, D. P. Fernandez, C. K. Jensen, and D. E. Schindler (2016), Dendritic network models: Improving isoscapes and quantifying influence of landscape and in-stream processes on strontium isotopes in rivers, *Geophys. Res. Lett.*, *43*, doi:10.1002/2016GL068904.

Received 5 FEB 2016
Accepted 29 APR 2016
Accepted article online 5 MAY 2016

Dendritic network models: Improving isoscapes and quantifying influence of landscape and in-stream processes on strontium isotopes in rivers

Sean R. Brennan[1], Christian E. Torgersen[2,3], Jeff P. Hollenbeck[2], Diego P. Fernandez[4], Carrie K. Jensen[5], and Daniel E. Schindler[1]

[1]School of Aquatic and Fishery Sciences, University of Washington, Seattle, Washington, USA, [2]Forest and Rangeland Ecosystem Science Center, Cascadia Field Station, U.S. Geological Survey, Corvallis, Oregon, USA, [3]School of Environmental and Forest Sciences, University of Washington, Seattle, Washington, USA, [4]Department of Geology and Geophysics, University of Utah, Salt Lake City, Utah, USA, [5]Department of Forest Resources and Environmental Conservation, Virginia Polytechnic Institute and State University, Blacksburg, Virginia, USA

Abstract A critical challenge for the Earth sciences is to trace the transport and flux of matter within and among aquatic, terrestrial, and atmospheric systems. Robust descriptions of isotopic patterns across space and time, called "isoscapes," form the basis of a rapidly growing and wide-ranging body of research aimed at quantifying connectivity within and among Earth's systems. However, isoscapes of rivers have been limited by conventional Euclidean approaches in geostatistics and the lack of a quantitative framework to apportion the influence of processes driven by landscape features versus in-stream phenomena. Here we demonstrate how dendritic network models substantially improve the accuracy of isoscapes of strontium isotopes and partition the influence of hydrologic transport versus local geologic features on strontium isotope ratios in a large Alaska river. This work illustrates the analytical power of dendritic network models for the field of isotope biogeochemistry, particularly for provenance studies of modern and ancient animals.

1. Introduction

Isotopic tracers are used widely to quantify spatial and temporal patterns in the transport and flux of matter across Earth's surface [*Bowen*, 2010]. Such patterns provide the foundation of numerous interdisciplinary applications aiming to discern connectivity within and among aquatic, terrestrial, and atmospheric systems [*Good et al.*, 2015], and the provenance, movement, and habitat use of organisms [*Hobson et al.*, 2010]. The underlying framework of these applications is in robust representations of environmental isotopic variation, both with respect to sources and associated isotopic effects during transport (mixing and fractionation). Those representations have been called isoscapes or isotopic landscapes [*Bowen*, 2010].

Most isoscapes have been constructed by integrating (i) process-oriented modeling based on known mechanisms producing isotopic variation (e.g., fractionation and radioactive decay) and (ii) statistical modeling to compute the relative effects of different covariates via regression analysis and taking advantage of spatial dependencies via geostatistical interpolation. The latter is particularly important in the generation of spatially continuous estimates of isotopic variation across landscapes. Although substantial advancements have been made in the development of isoscapes, two current limitations face the field with respect to aquatic systems. First, geostatistical interpolations used to predict isotope values at unsampled locations have been limited to Euclidean space (the closest straight-line distance between two sites). Second, a quantitative framework is lacking that is able to apportion the influence of in-stream processes (e.g., downstream transport) and processes driven by connectivity to landscape features on observed isotopic patterns (e.g., aridity, vegetation cover, or geology). Spatial dependency in Euclidean space is likely adequate for modeling isoscapes of atmospheric, terrestrial, and oceanic systems, but isotopic patterns in rivers may be defined by a combination of Euclidean patterns and those dependencies unique to the dendritic networks of rivers, such as downstream transport.

A new class of geostatistical models has been developed to account for the unique spatial relationships of dendritic networks [*Peterson and Ver Hoef*, 2010; *Ver Hoef and Peterson*, 2010] and is able to apportion variance among in-stream versus landscape driven processes [*Ganio et al.*, 2005; *McGuire et al.*, 2014]. Unlike classical

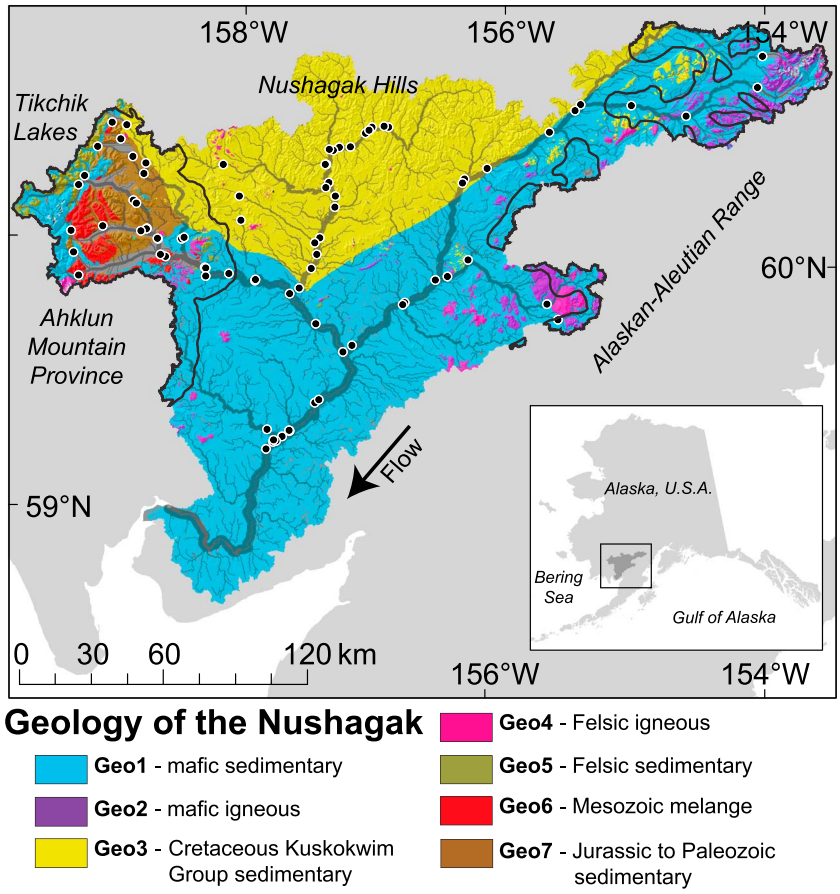

Figure 1. Geology of the Nushagak River. Black bold line indicates extent of most recent glaciation in the Nushagak basin. Black-filled circles indicate observation sites; width of streamlines is proportional to product of [Sr] and accumulated flow.

geostatistics, spatial stream network models (SSNMs) use autocovariance structures to account for the spatial dependences unique to rivers [*Isaak et al.*, 2014], such as the branching networks of streams, abrupt changes at confluences, direction of flow, and longitudinal connectivity of flowing water [*Peterson et al.*, 2013]. The application of these models to generate isoscapes of rivers has broad implications but has not yet been demonstrated. Here we show how SSNMs can be applied to improve the accuracy of riverine isoscapes and to discern the relative influence of in-stream processes versus landscape connectivity on isotopic patterns throughout rivers.

One tracer proven to be very useful in provenance and geochemical weathering research is strontium isotope ratios ($^{87}Sr/^{86}Sr$). Variation in $^{87}Sr/^{86}Sr$ has been used in a wide variety of contexts including discerning the relative influence of mantle-driven processes from continental weathering at millennia time scales on the composition of sea water [*Burke et al.*, 1982], reconstructing landscape use patterns of ancient hominids [*Copeland et al.*, 2011] and extinct megafauna [*Hoppe et al.*, 1999], and apportioning complex fishery harvests to distinct natal sources and life history strategies [*Brennan et al.*, 2015b; *Kennedy et al.*, 1997]. Current $^{87}Sr/^{86}Sr$ isoscapes [*Bataille et al.*, 2014] perform well at large continental spatial scales and at reproducing general patterns but poorly in geologically complex areas (e.g., metasedimentary regions). Their uncertainty is also relatively high ($\geq$0.0015) compared to the resolution relevant for many provenance applications (e.g., 0.0004 in *Brennan et al.* [2015b]). Improving the accuracy of $^{87}Sr/^{86}Sr$ river isoscapes, thus, has broad implications for provenance and geochemical weathering research.

To demonstrate the application of SSNMs for developing isoscapes and quantifying landscape versus in-stream driven processes on isotopic patterns in rivers, we applied these models to $^{87}Sr/^{86}Sr$ ratios in water throughout the Nushagak River in southwestern Alaska (Figure 1). $^{87}Sr/^{86}Sr$ ratios were temporally stable at subannual and interannual time scales within this watershed [*Brennan et al.*, 2015a], thus simplifying any interpretation of spatial patterns. We expected SSNMs to improve accuracy of predictions and that landscape features

would play a dominant role in shaping isotopic patterns (i.e., geologic heterogeneity) but would be modified by longitudinal transport as Sr is routed downstream through the network.

2. Materials and Methods

Estimating $^{87}Sr/^{86}Sr$ ratios in surface waters throughout the Nushagak River using SSNMs required (i) synthesizing multiple geospatial data products (Text S1 in the supporting information), including geologic maps, a digital elevation model (DEM), a network topology free of geometric errors, and measured $^{87}Sr/^{86}Sr$ and strontium concentrations (mg/L, referred to hereafter as [Sr]) values throughout the network, (ii) an SSNM of [Sr] throughout the network, (iii) an SSNM of $^{87}Sr/^{86}Sr$ ratios which incorporated the results from the model of [Sr] in the form of a spatial weighting scheme, (iv) identifying the best performing models, and (v) using this model to estimate $^{87}Sr/^{86}Sr$ ratios for each stream segment within the river network. All data analyses were conducted in R (http://cran.r-project.org/) using the Spatial Stream Network (SSN) package [*Ver Hoef et al*., 2014] and Spatial Tools for the Analysis of River Systems (STARS) toolbox in ArcGIS 10.2 [*Peterson and Ver Hoef*, 2014].

2.1. Spatial Linear Mixed Models

We used SSNMs to analyze a published water data set [*Brennan et al*., 2015a], with additional data (total $n = 86$ sites) describing $^{87}Sr/^{86}Sr$ ratios throughout the Nushagak River (Figure 1). Complete formulations of these models are described elsewhere [*Peterson and Ver Hoef*, 2010; *Ver Hoef and Peterson*, 2010]. Briefly, SSNMs use a moving average (MA) construction based on hydrologic distance, which is the shortest distance between any two points measured along the stream network. The branching nature of river systems requires the MA functions to split at stream junctions, and this is done by using spatial weighting schemes based on watershed features, such as upstream area or volume of flow. By using a mixed-effects modeling framework, SSNMs are able to account for the variance explained by a set of covariates as fixed effects (e.g., percent geology type) and the variance explained by different autocovariance functions as random effects. In addition to Euclidean autocorrelation, SSNMs can explicitly quantify the spatial dependence between flow-connected and flow-unconnected sites via "tail-up" and "tail-down" autocovariance structures, respectively [*Ver Hoef and Peterson*, 2010]. Tail-up models account for autocorrelation among flow-connected sites in an upstream direction. Tail-down models account for autocorrelation among flow-connected and flow-unconnected sites in a downstream direction. The general form of these spatial linear mixed models is

$$\mathbf{y} = \mathbf{X}\boldsymbol{\beta} + \mathbf{z}_{TU} + \mathbf{z}_{TD} + \mathbf{z}_{E} + \boldsymbol{\varepsilon}, \tag{1}$$

where $\mathbf{y}$ is the vector of the response variable ($^{87}Sr/^{86}Sr$ ratios or [Sr]), $\mathbf{X}$ is a matrix of covariates (e.g., percent geology types), $\boldsymbol{\beta}$ is a vector of the parameters for each covariate, $\mathbf{z}_{TU}$, $\mathbf{z}_{TD}$, and $\mathbf{z}_{E}$ are vectors of random variables with tail-up, tail-down, and Euclidean correlation structures, respectively, and $\boldsymbol{\varepsilon}$ is a vector of independent random errors.

2.2. Spatial Weights

SSNMs require spatial weights computed along the stream network to inform how the MA functions split at stream junctions. SSNMs use "segment proportional influence" to compute the relative influence of each stream segment on its downstream segment. A "segment" corresponds to the length of stream between two junctions within a river network. For example, if q denotes some watershed quantity measured at all segments, such as upstream area, and i and j are segments flowing into segment k, then SSNMs compute weights, ω_i, as $\omega_i = q_i/(q_i + q_j)$, and $\omega_j = q_j/(q_j + q_i)$ where $\omega_i + \omega_j = 1$, such that ω_i and ω_j denote the proportional influence of segments i and j on k based on upstream area. Commonly, SSNM spatial weights are based on watershed area. Other weighting schemes include using estimates of stream flow. As a proxy for flow, we used a gridded estimate of the decadal mean annual precipitation amount (mm) throughout the entire basin (Text S1) and accumulated these estimates at each river segment using the STARS toolbox in ArcGIS [*Peterson and Ver Hoef*, 2014]. In addition to the amount of water flowing past any location within the network, the reactivity of different geologic materials (e.g., carbonate minerals versus silicates) influence how much Sr is released into rivers. As such, we combined estimates of the precipitation and [Sr] in river water into one spatial weight defined as the product of these two parameters (Figure 1). Thus, to estimate $^{87}Sr/^{86}Sr$ ratios throughout the entire Nushagak River, we first used SSNMs to estimate [Sr] values throughout the network using precipitation to compute weights. We then used these estimates to calculate the spatial weights for

the $^{87}Sr/^{86}Sr$ model, defined as the product of [Sr] and precipitation from all upstream components of the watershed at a given site.

2.3. Predictors

To make this approach transferrable among systems, we used a set of simple covariates as predictors of $^{87}Sr/^{86}Sr$ ratios derived from commonly available geospatial data products (Table S1). The geology of the Nushagak basin was simplified into seven major groups based on lithology type and age (Figure 1 and Text S1). The percent area was computed for each lithological group contributing to all downstream locations throughout the catchment. Here these locations included "prediction sites" (the midpoint of each unique stream segment) and "observation sites" (Figure 1). Using the mixed-effects framework of SSNMs we fit equation (1) using observation sites. We compared multiple candidate models differing in fixed effects and autocovariance functions using AIC (Akaike information criterion: a measure of model performance by balancing trade-offs between overfitting and complexity). Multiple types of autocovariance functions for each spatial relationship were tested (e.g., exponential, spherical, and linear sill) available in the SSN R package [*Ver Hoef et al*., 2014]. After identifying the best model via AIC, we then estimated $^{87}Sr/^{86}Sr$ ratios at each prediction-site throughout the network.

To develop an SSNM for [Sr] throughout the Nushagak River, we tested additional predictors also known to influence geochemical weathering including relief and the watershed area recently glaciated (Table S1). We estimated relief using multiple metrics including percent slope and "local relief," which we define as the difference between the maximum and minimum elevations within each reach contributing area—the local basin area that contributes to each segment within the network. To evaluate the effect of recent glaciations, we computed the percent area upstream of each segment that was glaciated during the Late Wisconsin (Figure 1) [*Manley and Kaufman*, 2002].

2.4. Empirical Semivariograms

We used empirical semivariograms (ES), which describe spatial structure in [Sr] and $^{87}Sr/^{86}Sr$ ratios by calculating the semivariance (γ of observations as a function of distance (d), to analyze patterns in flow-connected, flow-unconnected, and Euclidean spatial relationships. ESs of the former two are referred to as Torgegrams, which illustrate the $\gamma(d)$ of each network relationship separately [*Peterson et al*., 2013]. Semivariance was calculated using the robust estimator of *Cressie* [1993] (as in *Ganio et al*. [2005]) and a lag class interval of 15 km; calculations of γ were based on $\geq$30 pairs of sample points [*Rossi et al*., 1992]. Torgegrams were evaluated visually based on the methods of *McGuire et al*. [2014] to identify broad scale, fine scale, or nested scales of heterogeneity in [Sr] and $^{87}Sr/^{86}Sr$ ratios.

2.5. Water Analyses

The additional water samples reported here ($n = 20$ sites) were collected, filtered, and acidified as in *Brennan et al*. [2014]. These samples came from the Tikchik Lakes region (Figure 1), a geologically complex area with the oldest and most chemically reactive (marine limestone) lithologies in the basin (Table S2). Water samples were analyzed for [Sr] and $^{87}Sr/^{86}Sr$ ratios using single and multicollector inductively coupled plasma mass spectrometry (Text S1).

3. Results

$^{87}Sr/^{86}Sr$ ratios from the 20 new sites ranged from 0.70477 to 0.71163 (Table S3), a 50% increase in the range of observed $^{87}Sr/^{86}Sr$ ratios in the Nushagak River basin [*Brennan et al*., 2015a]. [Sr] ranged from 0.0220 to 0.1462 mg/L; [Sr] in the field blank was below the limit of detection ($<$0.00003 mg/L). Standard deviations (2SD) of $^{87}Sr/^{86}Sr$ ratios and [Sr] of the field triplicate were ±0.00002 and ±0.0003 mg/L (King Salmon River), respectively, which is consistent with previous work in this watershed [*Brennan et al*., 2015a].

3.1. Multiscale Spatial Structure of $^{87}Sr/^{86}Sr$ and [Sr] Within the Nushagak

$^{87}Sr/^{86}Sr$ ratios and [Sr] showed multiscale spatial structure with respect to flow-connected, flow-unconnected, and Euclidean relationships (Figure 2). Torgegrams for both tracers showed evidence of fine-scale structure at $<$50–85 km, as indicated by consistent inflection points in γ at these distances; the fine-scale inflection points for flow-unconnected and Euclidean were more subtle for $^{87}Sr/^{86}Sr$ ratios. Flow-unconnected and Euclidean semivariograms also exhibited consistently higher and more variable γ

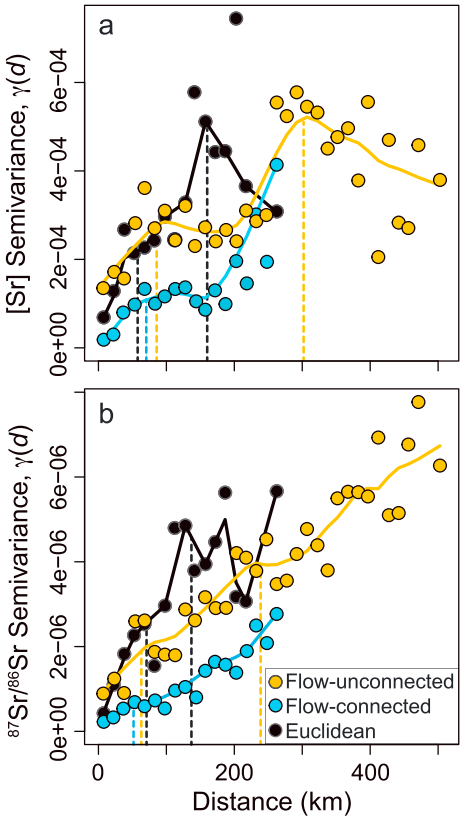

Figure 2. Semivariograms of (a) [Sr] and (b) $^{87}Sr/^{86}Sr$ ratios for the Nushagak basin, indicating nested spatial structure for flow-unconnected, flow-connected, and Euclidean relationships. Vertical dotted lines indicate fine- and broad-scale ranges visually determined by inflection points. Solid lines were smoothed to data using LOWESS (locally weighted scatterplot smoothing; smoothing factor = 1/3).

compared to flow-connected sites, especially at distances >150 km. Broad-scale spatial structure in [Sr] and $^{87}Sr/^{86}Sr$ was more variable, persisting to distances of 150 km for Euclidean relationships and >250 km for flow-connected and flow-unconnected relationships. These ranges also corresponded well with patch sizes for the geologic groups considered here (Table S1).

3.2. Model Results

The distribution of [Sr] exhibited positive skew, so data were log transformed before fitting models. The best model for predicting [Sr] throughout the Nushagak River included all geology types (Geo1–7), local relief, and the extent of the most recent glaciation as fixed effects (Figure 3a and Table S4). As random effects, this model included Epanechnikov tail-up [*Garreta et al.*, 2010] and Gaussian Euclidean autocovariance functions. Of all the models tested, the nonspatial model performed most poorly (ΔAIC = 70.9, the difference in AIC between a candidate model and the best model) and the model including only Euclidean autocovariance was also one of the lowest ranked (ΔAIC = 49.2). In the best model, the fixed effects explained 42.0% of variation (r^2) in [Sr], while the tail-up and Euclidean autocorrelation functions explained 38.7% and 17.5% of the variation, respectively (Table S5).

The best model for predicting $^{87}Sr/^{86}Sr$ ratios across the Nushagak River included three geology types (Table S6), $Geo3_{Kk}$, $Geo6_{Mzm}$, and $Geo7_{JPz\_carb\_seds}$ (Figure 3b). As random effects, it included Epanechnikov tail-up and exponential tail-down autocovariance functions. As with the [Sr] model, the nonspatial $^{87}Sr/^{86}Sr$ model performed the worst (ΔAIC = 51.6), and a model including only Euclidean autocovariance also performed poorly (ΔAIC = 48.9) (Table S6). In the best model, the fixed effects explained 70.5% of the variation in $^{87}Sr/^{86}Sr$, while the tail-up and tail-down autocorrelation models explained 22.9% and 4.4%, respectively (Table S7). Using leave-one-out cross validation, the root-mean-square prediction error (RMSPE) of the best model was 0.00051, and the r^2 of modeled versus observed ratios was 0.90 (Figure S1). The standard error (SE) of all predictions across the network ranged from 0.0002 to 0.0012 (Figure S2).

4. Discussion and Conclusions

By explicitly modeling the unique spatial structure of rivers, we generated an $^{87}Sr/^{86}Sr$ isocape that produced excellent fit to observations distributed throughout the watershed (RMSPE = 0.00051). We also identified multiscale spatial patterns of [Sr] and $^{87}Sr/^{86}Sr$ ratios in rivers via flow-connected, flow-unconnected, and Euclidean relationships, indicating interactive effects of landscape and in-stream processes on these constituents.

4.1. In-Stream and Landscape Processes Shape [Sr] and $^{87}Sr/^{86}Sr$ Ratios in Rivers

Flow-connected, flow-unconnected, and Euclidean relationships of $^{87}Sr/^{86}Sr$ ratios and [Sr] all exhibited nested spatial structure, where both broad-scale and fine-scale processes influenced these constituents

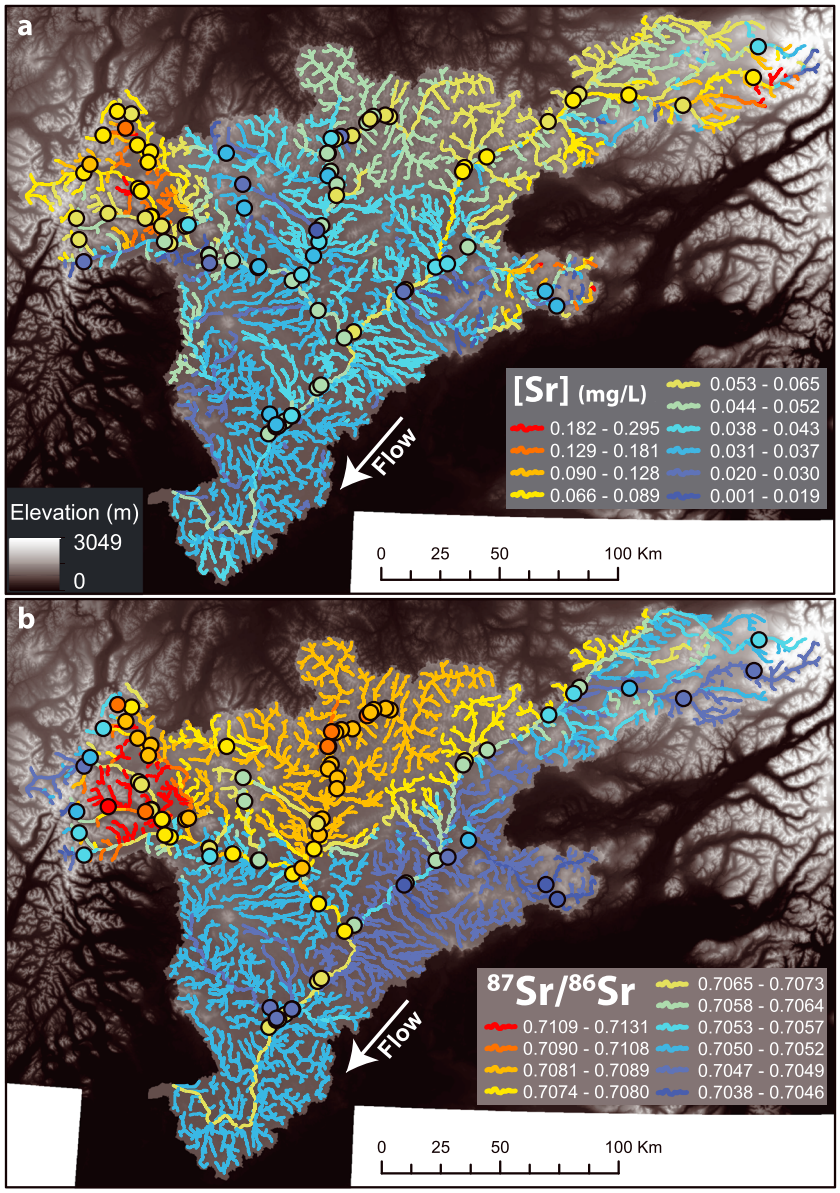

Figure 3. Predicted (a) [Sr] and (b) $^{87}Sr/^{86}Sr$ ratios across the Nushagak River. Colored circles indicate observations; colors of both circles and streams use the same breaks (natural breaks in data set; intervals > SE of prediction).

[*McGuire et al*., 2014]. Inspection of ESs provided insights into the degree of control by landscape and in-stream processes on observed patterns (Figure 2). Flow-connected relationships may indicate in-stream driven processes, i.e., longitudinal connectivity via downstream transport, whereas flow-unconnected and Euclidean relationships may reflect the influence of landscape features, including geology. Here flow connections consistently yielded lower variance as a function of distance compared to the other spatial relationships, illustrating the strong influence of longitudinal transport on $^{87}Sr/^{86}Sr$ and [Sr]. Strong coherence at fine spatial scales in the flow-unconnected and Euclidean semivariograms (Figure 2), and their similarly nested profiles, illustrates the influence of geologic heterogeneity across the landscape. The fine-scale structure, in the Torgegrams (<50–85 km), likely reflects abrupt changes occurring at stream confluences and geologic boundaries (faults). The large areas, or "patch sizes" (Table S1), of some geologic units likely drive broad-scale patterns. Thus, isotopic homogeneity is characteristic within units, which can correspond to broad ranges, whereas isotopic heterogeneity defines areas proximate to geologic boundaries at fine scales and at broad scales between discrete lithological units with large patch sizes.

The best $^{87}Sr/^{86}Sr$ model indicated that landscape processes explained 75% (fixed effects + tail down) of the variation, while 23% (tail up) was accounted for by longitudinal connectivity via hydrological transport. Incorporating Euclidean autocovariance did not improve the model, suggesting that the covariates of geology type accounted for Euclidean patterns. The tail-down autocovariance (explaining 4%) is likely due to similarities in landscape features located upstream of confluences sharing similar geology (range $<$ 150 km, Figure S3). Longitudinal connectivity explained the majority of the variance not explained by fixed effects (23%), reflecting the process of downstream routing of Sr through the river network and the mixing of isotopically different tributaries into higher-order reaches.

Landscape processes (fixed effects + Euclidean) explained less variation in the [Sr] model (60%) compared to the $^{87}Sr/^{86}Sr$ model, while longitudinal connectivity explained the remainder (tail up = 39%). The fact that fixed effects alone only explained 42%, while Euclidean patterns absorbed an additional 18%, suggests that geology-type, relief, and recent glaciation history were not sufficient at explaining all the landscape processes influencing spatial variation in [Sr]. Possible landscape features affecting [Sr] could be differences in the temperature effect on chemical weathering across the basin or vegetation cover via documented effects of interspecific differences on Sr cycling in boreal forests [*Poszwa et al*., 2004]. Nonetheless, the flexible mixed modeling framework of the SSNM was able to account for this variation by including Euclidean autocovariance. Similar to the isotope model, longitudinal connectivity was an important process shaping [Sr], explaining 39% of the variation.

4.2. SSNMs Improve Predictions of [Sr] and $^{87}Sr/^{86}Sr$ Ratios in Rivers

The RMSPE of the best $^{87}Sr/^{86}Sr$ model was almost an order of magnitude smaller than the process-oriented approach of *Bataille et al*. [2014] (RMSPE = 0.0045; if excluding four outliers = 0.0015). Comparing the *Bataille et al*. [2014] model to the SSNMs here requires caution, as the two models differ in spatial scale and also in the nature of their target predictions (prediction of each grid cell as in *Bataille et al*. [2014] versus each river segment within a network via SSNMs). However, metrics such as r^2 and RMSPE of their cross-validation tests provide some insight into the relative performance of these approaches, both of which show marked improvements for the SSNMs (Figure S1 and Tables 3 and 4) [*Bataille et al*., 2014]. Although caution is required when comparing cross-validation tests, from a modeling process standpoint, the SSNMs here also point out the advantages of accounting for the dendritic spatial structure of rivers and of making predictions at the level of stream segments versus grid cells when the goal is to analyze isotopic patterns throughout rivers.

To date, the general approach for generating $^{87}Sr/^{86}Sr$ isoscapes has been to estimate isotopic values at the "local" level (1 km grid cells) using a mixture of process-oriented and statistical methods and then to apply a flow accumulation model to represent values along a river network [*Bataille and Bowen*, 2012; *Bataille et al*., 2014]. To estimate local values, these efforts integrate bedrock geology and chemical weathering models. $^{87}Sr/^{86}Sr$ ratios of bedrock are estimated as a function of rock age, rock type, and also the recycling history of siliclastic sediments during the tectonic evolution of geologic terranes [*Bataille et al*., 2014]. The only statistical aspects of this formulation are the geostatistical interpolations used to compute the needed parameters for the $^{87}Sr/^{86}Sr$ evolution equations of bedrock at all locations. The chemical weathering portion of the *Bataille et al*. [2014] model is primarily statistical, using a multiple regression to predict [Sr] at all locations as a function of lithology type and other parameters, such as slope and permafrost. To represent the isotopic composition of river networks, a flow accumulation model is then applied to these local estimates using a DEM and gridded estimates of precipitation via ArcGIS's "Flow Accumulation" tool (Spatial Analyst Toolbox) [*Bataille et al*., 2014].

Implicit in such approaches is that the model accurately predicts local isotope values and there is no modification of isotope values during transport. Although the latter may be valid for conservative constituents such as [Sr] and $^{87}Sr/^{86}Sr$, the former is likely not valid at all locations. In primarily igneous terranes, predictions of $^{87}Sr/^{86}Sr$ perform well, due to accurate dating techniques and the known half-life of ^{87}Rb. However, sedimentary and metamorphic processes, which reconstitute and mix multiple source rock materials, pose difficult challenges to process-oriented approaches, as is evident by significant reductions in performance of sedimentary bedrock models [*Bataille and Bowen*, 2012; *Bataille et al*., 2014] and the significant deviations of river water predictions in metamorphic regions [*Bataille et al*., 2014].

The primarily statistical approach of SSNMs outlined here allows predictions of stream segments to be based on known drivers of isotopic variation (bedrock heterogeneity and differential chemical weathering), but not restricted by deterministic estimates at each local grid cell. Thus, in SSNMs the effects of covariates are calibrated to regional and local conditions and what is not explained by covariates can be incorporated via different spatial autocovariance functions. The importance of network and Euclidean spatial structure is particularly evident in the ESs of both tracers after the fixed effects have been fit to the data (Figure S3), all of which show spatial dependence. Furthermore, the utility of SSNMs is not limited to solely generating isoscapes. Rather, SSNMs also yield unique insights into the elusive interplay between in-stream and landscape processes driving isotopic patterns in rivers.

The limitations of the SSNM approach include the need for a spatially representative data set and a topologically correct network. The SE of predictions from SSNMs are sensitive to the sampling distribution throughout a study region, where extrapolation yields larger errors than interpolation (Figure S2). Thus, it is important to obtain observations in both headwater and downstream regions. Provenance and geochemical weathering studies, however, require sampling surveys that span the topological and geological variation expressed across watersheds. As the use of SSNMs grows, and improvements to hydrography data sets and DEMs accumulate, topologically correct networks will be easier to obtain. Coupling SSNMs with process-oriented approaches should lead to better predictions and insights into isotopic patterns at fine to continental scales.

4.3. Implications for Other Isotope Systems

SSNMs have broad implications for the analysis and prediction of spatial patterns of other isotope systems in rivers. For example, similar to the more process-oriented $^{87}Sr/^{86}Sr$ isoscapes, the best performing δ^2H and $\delta^{18}O$ river isoscapes apply a flow accumulation model to gridded estimates of precipitation isotope values [*Bowen et al*., 2011]. However, the same implicit assumptions apply because these model formulations assume that local predictions are accurate and there is no isotopic modification during transport. For the stable isotope systems of $^2H/^1H$ and $^{18}O/^{16}O$, these assumptions are not likely met, particularly the latter at all locations along a flow path. River isoscapes of δ^2H and $\delta^{18}O$ generated using flow accumulation models perform quite well, but they also exhibit systematic biases in predictions. These biases may be due to evaporative effects on the isotopic composition of waters during transport or to the relative influence of transpiration across basins [*Bowen et al*., 2011]. SSNMs provide a viable framework to quantify these effects separately. Furthermore, final isoscape surfaces produced via these formulations incorporate a "residual correction" step, whereby a Euclidean geostatistical model is used to interpolate between observed residuals, which are subtracted from the original model. Because SSNMs account for flow-connected and flow-unconnected spatial dependencies of river networks, their predictions will likely be more accurate than nonspatial models or those based solely on Euclidean distance (Tables S4 and S6). SSNMs may minimize the need for circular residual corrections, or if needed, will make the interpolated residual surface more accurate by accounting for network relationships.

4.4. Implications for Provenance Studies

The ability to generate accurate $^{87}Sr/^{86}Sr$ isoscapes has important implications for provenance research. The uncertainty of current Sr isoscapes [*Bataille et al*. [2014]] represents an isotopic range potentially meaningful to a variety of provenance investigations. For example, $^{87}Sr/^{86}Sr$ ratios were used to assign adult Chinook salmon caught in a coastal fishery back to seven natal regions in the Nushagak River; the 2SD of each natal region was ±0.0004 [*Brennan et al*., 2015b]. Further, nearly 50% of the Earth's surface, and 70% of Alaska's, is composed of siliclastic sedimentary rocks [*Hartmann and Moosdorf*, 2012]. Because current process-oriented models indicate reduced performance in these geologically complex regions, application of SSNMs in these areas will refine applications of isoscapes to provenance research. For example, the eastern interior of Alaska is defined by metasedimentary lithologies, where predicted river $^{87}Sr/^{86}Sr$ ratios exhibit large deviations from observed [*Bataille et al*., 2014]. Interior Alaska supports several species of Pacific salmon and was also ice free during the last glaciation, providing important refugia for ancient humans [*Potter et al*., 2011] and extinct megafauna [*Guthrie*, 2006]. The radiogenic composition of the eastern interior defines a strong east-west isotopic gradient within this corridor. Accurately characterizing such a gradient will provide a viable framework to discern migrations of ancient and modern animal populations.

Acknowledgments
The Bristol Bay Regional Seafood Association and Bristol Bay Science Research Institute funded this research. Alaska Sea grant R/100-02 funded non-Tikchik Lake [Sr] analyses. Thanks to Christine Woll and the Alaska Chapter of The Nature Conservancy for work on the Nushagak River topology; Erin Peterson, Jay Ver Hoef, Daniel Isaak, Jeff Falke, and David Hockman-Wert for training in STARS/SSN; Gabriel Bowen and the SPATIAL Short Course faculty at the University of Utah for training and financial support of SRB to attend course; Adrianne Smits for help with fieldwork; Clement Bataille for his helpful discussions; two anonymous reviewers and Christian Zimmerman. Any use of trade, product, or firm names is for descriptive purposes only and does not imply endorsement by the U.S. government. Data used are listed in the supporting information.

References

Bataille, C. P., and G. J. Bowen (2012), Mapping Sr-87/Sr-86 variations in bedrock and water for large scale provenance studies, *Chem. Geol.*, *304*, 39–52.

Bataille, C. P., S. R. Brennan, J. Hartmann, N. Moosdorf, M. J. Wooller, and G. J. Bowen (2014), A geostatistical framework for predicting variations in strontium concentrations and isotope ratios in Alaskan rivers, *Chem. Geol.*, *389*, 1–15.

Bowen, G. J. (2010), Isoscapes: Spatial pattern in isotopic biogeochemistry, *Annu. Rev. Earth Planet. Sci.*, *38*(38), 161–187.

Bowen, G. J., C. D. Kennedy, Z. F. Liu, and J. Stalker (2011), Water balance model for mean annual hydrogen and oxygen isotope distributions in surface waters of the contiguous United States, *J. Geophys. Res.*, *116*, G04011, doi:10.1029/2010JG001581.

Brennan, S. R., D. P. Fernandez, G. Mackey, T. E. Cerling, C. P. Bataille, G. J. Bowen, and M. J. Wooller (2014), Strontium isotope variation and carbonate versus silicate weathering in rivers from across Alaska: Implications for provenance studies, *Chem. Geol.*, *389*, 167–181.

Brennan, S. R., D. P. Fernandez, C. E. Zimmerman, T. E. Cerling, R. J. Brown, and M. J. Wooller (2015a), Strontium isotopes in otoliths of a non-migratory fish (slimy sculpin): Implications for provenance studies, *Geochim. Cosmochim. Acta*, *149*, 32–45.

Brennan, S. R., C. E. Zimmerman, D. P. Fernandez, T. E. Cerling, M. V. McPhee, and M. J. Wooller (2015b), Strontium isotopes delineate fine-scale natal origins and migration histories of Pacific salmon, *Sci. Adv.*, *1*(4e1400124), doi:10.1126/sciadv.1400124.

Burke, W. H., R. E. Denison, E. A. Hetherington, R. B. Koepnick, H. F. Nelson, and J. B. Otto (1982), Variation of seawater $^{87}Sr/^{86}Sr$ throughout Phanerozoic time, *Geology*, *10*, 516–519.

Copeland, S. R., M. Sponheimer, D. J. de Ruiter, J. A. Lee-Thorp, D. Codron, P. J. le Roux, V. Grimes, and M. P. Richards (2011), Strontium isotope evidence for landscape use by early hominins, *Nature*, *474*(7349), 76–78, doi:10.1038/nature10149.

Cressie, N. A. C. (1993), *Statistics for Spatial Data*, Rev. ed., 900 pp., Wiley, New York.

Ganio, L. M., C. E. Torgersen, and R. E. Gresswell (2005), A geostatistical approach for describing spatial pattern in stream networks, *Front. Ecol. Environ.*, *3*(3), 138–144.

Garreta, V., P. Monestiez, and J. M. Ver Hoef (2010), Spatial modelling and prediction on river networks: Up model, down model or hybrid?, *Environmetrics*, *21*(5), 439–456.

Good, S. P., D. Noone, and G. Bowen (2015), Hydrologic connectivity constrains partitioning of global terrestrial water fluxes, *Science*, *349*(6244), 175–177.

Guthrie, R. D. (2006), New carbon dates link climatic change with human colonization and Pleistocene extinctions, *Nature*, *441*(7090), 207–209.

Hartmann, J., and N. Moosdorf (2012), The new global lithological map database GLiM: A representation of rock properties at the Earth surface, *Geochem. Geophys. Geosyst.*, *13*, Q12004, doi:10.1029/2012GC004370.

Hobson, K. A., R. Barnett-Johnson, and T. E. Cerling (2010), Using isoscapes to track animal migration, in *Isoscapes: Understanding Movement, Pattern, and Process on Earth Through Isotope Mapping*, edited by J. B. West et al., pp. 273–298 , Springer, Netherlands.

Hoppe, K. A., P. L. Koch, R. W. Carlson, and S. D. Webb (1999), Tracking mammoths and mastodons: Reconstruction of migratory behavior using strontium isotope ratios, *Geology*, *27*(5), 439–442.

Isaak, D. J., et al. (2014), Applications of spatial statistical network models to stream data, *WIREs Water*, *1*, 277–294.

Kennedy, B. P., C. L. Folt, J. D. Blum, and C. P. Chamberlain (1997), Natural isotope markers in salmon, *Nature*, *387*(6635), 766–767.

Manley, W. F., and D. S. Kaufman (2002), *Late Wisconsin Glacier Extents, Alaska PaleoGlacier Atlas version 1*, Univ. of Colo., Institute of Arctic and Alpine Research (INSTAAR). [Available at http://instaar.colorado.edu/QGISL/ak_paleoglacier_atlas.]

McGuire, K. J., C. E. Torgersen, G. E. Likens, D. C. Buso, W. H. Lowe, and S. W. Bailey (2014), Network analysis reveals multiscale controls on streamwater chemistry, *Proc. Natl. Acad. Sci. U.S.A.*, *111*(19), 7030–7035.

Peterson, E. E., and J. M. Ver Hoef (2010), A mixed-model moving-average approach to geostatistical modeling in stream networks, *Ecology*, *91*(3), 644–651.

Peterson, E. E., and J. M. Ver Hoef (2014), STARS: An ArcGIS toolset used to calculate the spatial information needed to fit spatial statistical models to stream network data, *J. Stat. Software*, *56*(2), 1–17.

Peterson, E. E., et al. (2013), Modelling dendritic ecological networks in space: An integrated network perspective, *Ecol. Lett.*, *16*(5), 707–719.

Poszwa, A., B. Ferry, E. Dambrine, B. Pollier, T. Wickman, M. Loubet, and K. Bishop (2004), Variations of bioavailable Sr concentration and Sr-87/Sr-86 ratio in boreal forest ecosystems—Role of biocycling, mineral weathering and depth of root uptake, *Biogeochemistry*, *67*(1), 1–20.

Potter, B. A., J. D. Irish, J. D. Reuther, C. Gelvin-Reymiller, and V. T. Holliday (2011), A terminal Pleistocene child cremation and residential structure from eastern Beringia, *Science*, *331*(6020), 1058–1062.

Rossi, R. E., D. J. Mulla, A. G. Journel, and E. H. Franz (1992), Geostatistical tools for modeling and interpreting ecological spatial dependence, *Ecol. Monogr.*, *62*(2), 277–314.

Ver Hoef, J. M., and E. E. Peterson (2010), A moving average approach for spatial statistical models of stream networks, *J. Am. Stat. Assoc.*, *105*(489), 6–18.

Ver Hoef, J. M., E. E. Peterson, D. Clifford, and R. Shah (2014), SSN: An R package for spatial statistical modeling on stream networks, *J. Stat. Software*, *56*(3), 1–45.